Available online at www.sciencedirect.com
ScienceDirect
Physica B 400 (2007) 66–69
PHYSICA B
www.elsevier.com/locate/physb

Manganite-layer thickness-dependent photovoltaic effect of $La_{0.9}Sr_{0.1}MnO_3/SrNb_{0.01}Ti_{0.99}O_3$ *p–n* heterojunction

Jie Qiu, Hui-Bin Lu, Kui-Juan Jin*, Meng He, Jie Xing

Beijing National Laboratory for Condensed Matter Physics, Institute of Physics, Chinese Academy of Sciences, Beijing 100080, China

Received 31 March 2007; received in revised form 8 June 2007; accepted 26 June 2007

Abstract

The perovskite *p–n* heterojunctions were fabricated by depositing $La_{0.9}Sr_{0.1}MnO_3$ (LSMO) layers with thicknesses ranging from 20 to 400 Å on $SrNb_{0.01}Ti_{0.99}O_3$ (SNTO) single-crystal substrates by laser molecular beam epitaxy (laser-MBE). The open-circuit photovoltage of the LSMO/SNTO heterojunction at room temperature increases with the increase of the thickness of LSMO layer. This result is ascribed to the increase of the carrier amount and the enhancement of the built-in electric field in the space-charge region of the LSMO/SNTO heterojunction with the increase of the thickness of LSMO layer. Furthermore, we found that the speed of photovoltaic response is almost independent of the thickness of LSMO layer in the heterojunction.

PACS: 73.40.Lq; 72.40.+w; 85.30.Kk

Keywords: Heterojunctions; Photovoltaic effects; Junction diodes

1. Introduction

Perovskite manganite oxides are well known for the phenomenon of colossal magnetoresistance [1–4]. Recently, oxide *p–n* junctions based on manganites also have attracted considerable attention because of their potential applications and some interesting physical phenomena like positive colossal magnetoresistance [5], photocarrier injection effect [6] and rectification characteristics [7].

Picosecond photoelectric characteristic in $La_{0.7}Sr_{0.3}MnO_3$/Si *p–n* junctions [8], lateral photovoltaic effect in *p–n* junctions of $La_{0.7}Sr_{0.3}MnO_3$ and Si [9] and the photoelectric characteristic of $La_{0.9}Sr_{0.1}MnO_3$ (LSMO)/$SrNb_{0.01}Ti_{0.99}O_3$ (SNTO) *p–n* junction [10] were reported. Moreover, Luo and Gao further investigated the effect of the supplied power of lamp and temperature on the photovoltage of LSMO/SNTO heterostructrue [11]. These works mainly focused on the photovoltaic effect of oxide *p–n* junctions with LSMO thin films. To understand physical mechanisms of the above complicated system, it would be necessary to investigate the photovoltage effect of oxide *p–n* junctions with *ultrathin* LSMO layers. In this work, we present thickness-dependent photovoltage effect of all-oxide *p–n* junctions consisting of ultrathin LSMO layer, a p-type semiconductor with a band gap of about 1.0 eV, and 0.5-mm-thick SNTO substrate, an n-type semiconductor with a band gap of about 3.2 eV. We found that the maximum photovoltage of the LSMO/SNTO heterojunction increases with the increase of the thickness of LSMO layer.

2. Experimental

The LSMO/SNTO *p–n* junctions were fabricated by growing LSMO films with various thicknesses on SNTO (0 0 *l*) substrates by laser molecular beam epitaxy (laser-MBE). The growing process of LSMO layers was in situ monitored by reflection high-energy electron diffraction (RHEED). One period in the RHEED intensity oscillations marks the completion of one unit cell. So the thickness of LSMO ultrathin films was accurately controlled by the growth time which represented the number of the periods of the RHEED intensity oscillations. The detailed growth

*Corresponding author. Tel./fax: +86 10 82648099.
E-mail address: kjjin@aphy.iphy.ac.cn (K.-J. Jin).

0921-4526/$ - see front matter © 2007 Elsevier B.V. All rights reserved.
doi:10.1016/j.physb.2007.06.023

process and the RHEED intensity oscillations from the growth of LSMO ultrathin films were shown elsewhere [12]. The transport property of the LSMO/SNTO heterojunction with 40-Å-thick LSMO layer was measured with a pulse-modulated current source at room temperature. The photovoltages of the LSMO/SNTO heterojunctions excited by a XeCl pulsed laser (wavelength of 308 nm, repetition rate of 1 Hz and duration of 20 ns) were measured by a 500 MHz oscilloscope at room temperature after indium electrodes were placed on the LSMO surface and the opposite surface of SNTO, respectively. In order to calculate the built-in electric field in the space-charge region of the LSMO/SNTO heterojunction with thin LSMO layer, we self-consistently solved the Poisson's equation and the continuity equations under a steady state [13].

3. Results and discussion

A bright RHEED pattern of the ultrathin LSMO film with the thickness of 40 Å (shown in the bottom inset of Fig. 1) indicates that the LSMO layer has a good crystallized structure and a smooth surface. The current–voltage curve of the LSMO/SNTO heterojunction with 40-Å-thick LSMO layer at room temperature shows a rectifying property of a *p–n* junction as shown in Fig. 1.

Fig. 2 shows that the maximum open-circuit photovoltage was about 2, 13, 17 and 21 mV for the LSMO/SNTO heterojunctions with LSMO thicknesses of 20, 40, 200 and 400 Å, respectively. The photovoltage increases with the increase of the thickness of the LSMO layer, which can be understood as follows.

When the *p–n* junction is illuminated with laser pulse with photon energy (4.0 eV) larger than the band gap of the compounds of the *p–n* junction, the photons will be absorbed. The photon absorption coefficient α can be described as follows [14]:

$$\alpha = \frac{1}{c}\sqrt{\frac{1}{\rho^2 \varepsilon_r \varepsilon_0^2}}, \quad (1)$$

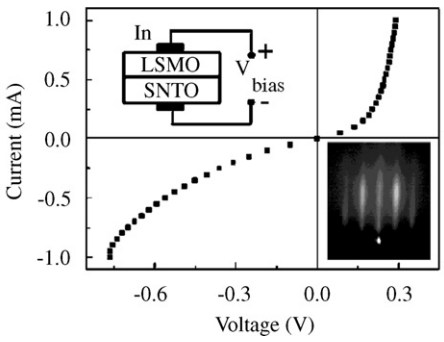

Fig. 1. The transport property of the LSMO/SNTO heterojunction with 40-Å-thick LSMO layer at room temperature. Top inset: schematic measurement circuit. Bottom inset: the RHEED pattern of 40-Å-thick LSMO layer.

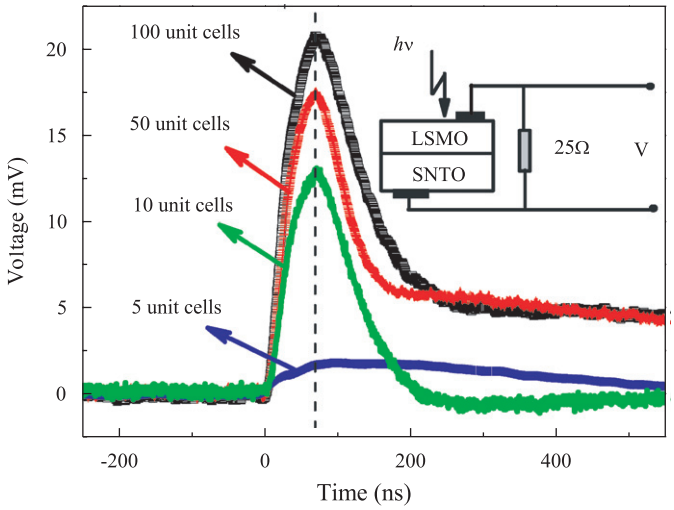

Fig. 2. The open-circuit photovoltage as a function of time to LSMO/SNTO *p–n* junctions. The inset presents the schematics of the measurement circuit.

where ρ is the material resistivity (2.866 Ω cm for LSMO and 1.84×10^{-3} Ω cm for SNTO) and ε_r denotes the relative dielectric constant (10 for LSMO and 150 for SNTO). The parameters c and ε_0 are the speed of light and the permittivity of free space, respectively. Then, the photon absorption coefficient is about 0.416 μm^{-1} for the LSMO compound and 0.167×10^4 μm^{-1} for the SNTO compound, respectively, by resolving Eq. (1). From the above estimated absorption coefficients of LSMO and SNTO compounds, we know that some photons are absorbed by SNTO substrate after transferring through LSMO layer for our samples.

According to Ref. [5] and the above analysis, we drew the schematics of the carrier movements and the band structures of the LSMO/SNTO heterostructures as shown in Fig. 3. The photons with energy greater than E_g will be absorbed by the valence electrons, and make them transition into the conduction band shown as the process 1 in Fig. 3. Thus, incident photons create electron–hole pairs in the space-charge region of the heterostructure. The excited electrons of the conduction band in the p region (LSMO) will be transferred into the n region (SNTO), and the holes of the valence band in the n region also will be transferred into the p region by the built-in electric field in the depletion layer of the *p–n* junction shown as the process 2 in Fig. 3. So a photocurrent is produced in the reverse-bias direction, and a photovoltage is produced in the forward-bias direction of the *p–n* junction.

The calculated results of the built-in electric field around the space-charge region of the LSMO/SNTO heterojunction with 400-Å-thick LSMO layer are shown by the solid line in Fig. 4. The calculated absolute value of the built-in electric field at the interface of the heterostructure is about 47.1 kV mm^{-1}. The corresponding built-in electric filed for the LSMO/SNTO heterojunction with 200-Å-thick LSMO layer is also schematically plotted as a dotted line in Fig. 4.

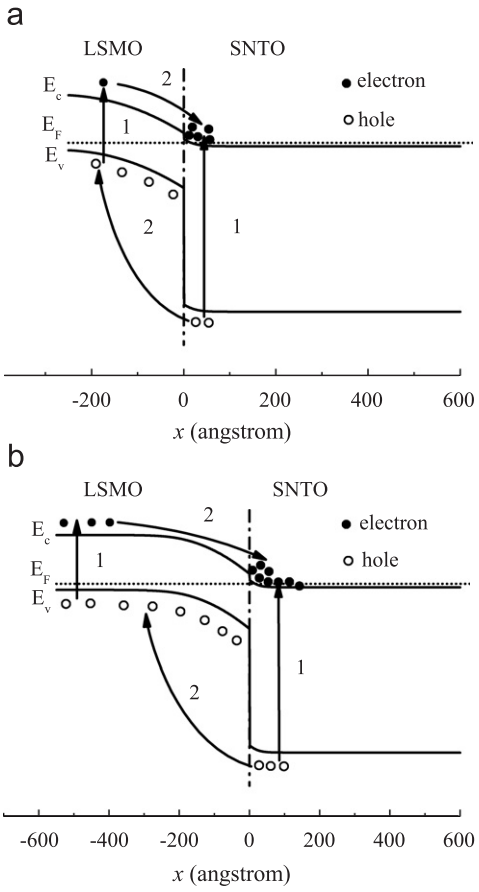

Fig. 3. Schematics of the carrier movements and the band structures for the LSMO/SNTO heterostructure with ultrathin LSMO layer (a) and that with thin LSMO layer (b). The horizontal axes represent the coordinates around the space-charge region in the growth direction.

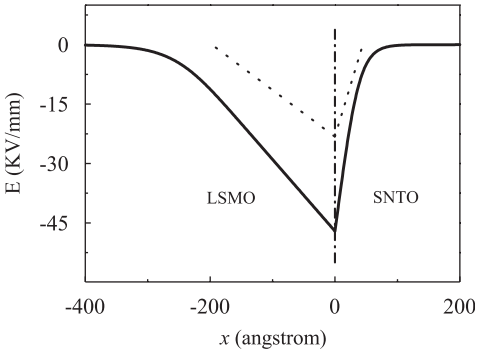

Fig. 4. Calculated electric field in the space-charge region of the LSMO/SNTO heterojunction with 400-Å-thick LSMO layer (identified by the solid line). The dotted line represents schematic electric field of the LSMO/SNTO heterojunction with 200-Å-thick LSMO layer. The vertical dash-dotted line denotes the interface of the LSMO/SNTO heterojunction.

The built-in electric field decreases with the decrease of the thickness of the LSMO layer as shown in Fig. 4, and the amount of transferred carriers should decrease correspondingly with the decreasing thickness of the LSMO layer. As a result, the photoelectric voltage increases with the increasing thickness of the LSMO layer, which is shown in Fig. 5 clearly. Except for the sample with the thinnest LSMO film, the photovoltage of LSMO/SNTO heterojunction increased linearly from 13 to 21 mV when the thickness of the LSMO ultrathin film increased from 40 to 400 Å.

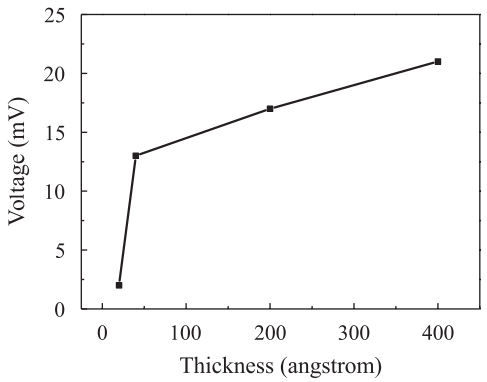

Fig. 5. Thickness-dependent photovoltage of LSMO/SNTO *p–n* junctions.

In Fig. 5, the non-linear decrease of photoelectric voltage of the thinnest film is obvious and interesting. We think it may be somehow related with the stronger interface effect for the thinner film. The interface state of the LSMO/SNTO heterojunction and the strain from the lattice mismatch between LSMO ultrathin film and SNTO substrate should play a more important role for the thinnest film [11]. And these effects may further reduce the built-in electric field of the *p–n* junction, which is the main reason why the photovoltage of the LSMO/SNTO heterostructure with the thinnest LSMO layer deviated from linearity and dropped sharply to 2 mV (shown in Fig. 5). Therefore, we believe these interface effects and the strain should be another reason for the thickness-dependent photovoltaic effect. It also should be noted that all the heterostructures with LSMO layers of various thicknesses almost have the same rise time of 70 ns, which means they almost have the same speed of photovoltaic response and the thickness of LSMO layer has little effect on the photovoltaic response time.

4. Conclusions

In summary, the LSMO-layer thickness-dependent photovoltaic effect of the LSMO/SNTO heterojunction was investigated. The photovoltage increases with the increase of the thickness of the LSMO layer, which is ascribed to the increase of the carrier amount of the LSMO layer and the enhancement of the built-in electric field in the space-charge region of the LSMO/SNTO heterojunction. This result should be helpful to understand the photovoltaic characteristics of the complex perovskite oxide materials. We also expect some potential applications of all-oxide *p–n* heterojunction in future microelectronic devices, and our results can provide necessary information for making electronic devices like photodetectors.

Acknowledgments

This work was supported by National Natural Science Foundation of China and National Basic Research Program of China no. 2007CB307000.

References

[1] S. Jin, T.H. Tiefel, M. Mccormack, R.A. Fastnact, R. Ramesh, L.H. Chen, Science 264 (1994) 413.
[2] R.V. Helmolt, J. Weeker, B. Holzapfel, K. Samwer, Phys. Rev. Lett. 71 (1993) 2331.
[3] C. Zener, Phys. Rev. 82 (1951) 403;
A.J. Millis, Nature 392 (1998) 147.
[4] J.B. Goodenough, J.S. Zhou, Nature 386 (1997) 229;
J.D. Zhang, P.C. Dai, F. Baca, E.W. Plummer, Y. Tomioka, Y. Tokura, Phys. Rev. Lett. 86 (2001) 3823.
[5] K.J. Jin, H.B. Lu, Q.L. Zhou, K. Zhao, B.L. Cheng, Z.H. Chen, Y.L. Zhou, G.Z. Yang, Phys. Rev. B 71 (2005) 184428;
H.B. Lu, S.Y. Dai, Z.H. Chen, Y.L. Zhou, B.L. Cheng, K.J. Jin, L.F. Liu, G.Z. Yang, X.L. Ma, Appl. Phys. Lett. 82 (2005) 032502.
[6] H. Katsu, H. Tanaka, T. Kawai, Appl. Phys. Lett. 76 (2000) 22.
[7] K. Lord, D. Hunter, T.M. Williams, A.K. Pradhan, Appl. Phys. Lett. 89 (2006) 052116;
T. Muramatsu, Y. Muraoka, Z. Hiroi, Solid State Commun. 132 (2004) 351.
[8] H.B. Lu, K.J. Jin, Y.H. Huang, M. He, K. Zhao, B.L. Cheng, Z.H. Chen, Y.L. Zhou, S.Y. Dai, G.Z. Yang, Appl. Phys. Lett. 86 (2005) 241915;
Z.G. Sheng, B.C. Zhao, W.H. Song, Y.P. Sun, J.R. Sun, B.G. Shen, Appl. Phys. Lett. 87 (2005) 244501.
[9] H.F. Tian, J.R. Sun, H.B. Lu, K.J. Jin, H.X. Yang, H.C. Yu, J.Q. Li, Appl. Phys. Lett. 87 (2005) 164102.
[10] H.Y. Huang, H.B. Lu, M. He, K. Zhao, Z.H. Chen, B.L. Chen, Y.L. Zhou, K.J. Jin, S.Y. Dai, G.Z. Yang, Sci. China, Ser. G 48 (2005) 381;
H.Y. Huang, K.J. Jin, K. Zhao, H.B. Lu, M. He, Z.H. Chen, Y.L. Zhou, G.Z. Yang, X.L. Ma, Chin. Phys. Lett. 23 (2006) 982.
[11] Z. Luo, J. Gao, J. Appl. Phys. 100 (2006) 056104.
[12] M. He, J. Qiu, X. Liang, H.B. Lu, K.J. Jin, Appl. Surf. Sci. 253 (2007) 6080.
[13] Q.L. Zhou, K.J. Jin, H.B. Lu, P. Han, Z.H. Chen, K. Zhao, Y.L. Liang, G.Z. Yang, Europhys. Lett. 71 (2005) 283.
[14] Y.H. Shen, W.Z. Zhu, Semiconductor Photovoltaic Characteristics, Xiamen University Press, Fujian Province, 1995, pp. 3–5.